LHCb Collaboration LHCb 2001-019 VELO
9th March 2001

The material distribution in a realistic VELO design

J. Libby, T. Ruf
CERN
M. McCubbin
University of Liverpool

Abstract

The realistic design of the VELO, implemented in `SICB`, has been used to determine the material distribution traversed by particles before entering the remainder of the LHCb spectrometer. In the range of polar angles, 8 mrad $\leq \theta \leq$ 270 mrad, the mean X_0 traversed, at the exit of the vertex tank, was found to be 18.9% of an X_0. The contributions of the different components of the VELO are given for both the total and different regions of the acceptance phase space. The impact of alternative designs on the material distribution is discussed.

1 Introduction

A more realistic RF–shield design, together with the overall optimisation of the VELO system [1] leads to an increase in the amount of material compared to the Technical Proposal (TP) design [2]. The material increase leads to greater occupancy in the downstream detectors due to secondary particle production in the VELO. The effect of this increased occupancy on pattern recognition and reconstruction was not considered in the optimisation procedure. This note presents an investigation into the material distribution in the VELO using the latest `GEANT` [3] description in `SICB`.

This note is organised as follows. In Section 2 the latest VELO design is described along with a description of its simulation in `GEANT`; the material profiles of the different VELO components are also given. In Section 3 the mean X_0 traversed by particles within the acceptance is presented. In addition, the contributions of the VELO components are given for the total and for regions of acceptance phase space. Certain particle trajectories which traverse up to 70% of an X_0 are explained in Section 4. Possible alterations to the VELO which reduce the material traversed will be discussed in Section 5. The conclusions are given in Section 6.

2 The realistic VELO design and its `GEANT` description

Following the simulation studies described in [1] the VELO geometry was changed from the TP design [2], which had 17 silicon stations, to a design with 25 stations. The silicon inner and outer radii were reduced. The baseline silicon sensor thickness has also increased from 150 μm to 300 μm [4]. A more realistic RF–shielding was included in the geometry description in the form of a special shaped aluminium foil of 250 μm thickness. This replaced the 100 μm thick aluminium foil that surrounded each half–station in the TP design. In addition, a thin-walled aluminium box was introduced which separates the primary and secondary vacua and more realistic supports for the silicon have also been implemented in `GEANT`. Some more details are given below and in [5].

The following gives a brief description of the `GEANT` volumes and how they are related to the physical objects they represent. All the VELO volumes are contained in the logical volume `SMVD`. The volumes describing the silicon, hybrids, supports and the RF–shielding are all daughters of the volume `VSVV`[1]. `VSVV` itself is placed in the volume `SMVD` which also contains the description of the vacuum tank and the first part of the vacuum pipe.

2.1 The silicon

The silicon detector shapes are represented by volumes `VSRP`, for the VELO, and `VPRP` for the VETO counters. In fact, the VETO counters are just a copy of the VELO r-detectors; these are only traversed by backward tracks. Each VELO station comprises two layers of silicon in the form of disks, the r and ϕ layers, with the left–side and right–side offset in z by 1.5 cm. The details of these volumes are given in Table 1.

[1] All 4 letter `GEANT` codes used to name volumes in `SICB` are written in typescript

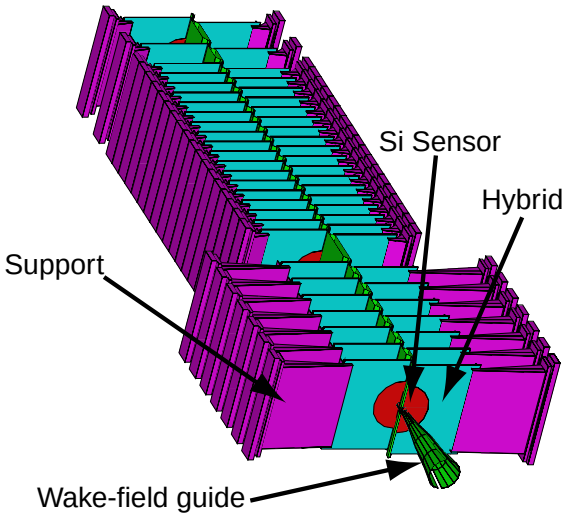

Figure 1: The supports, hybrid and silicon sensors of the VELO.

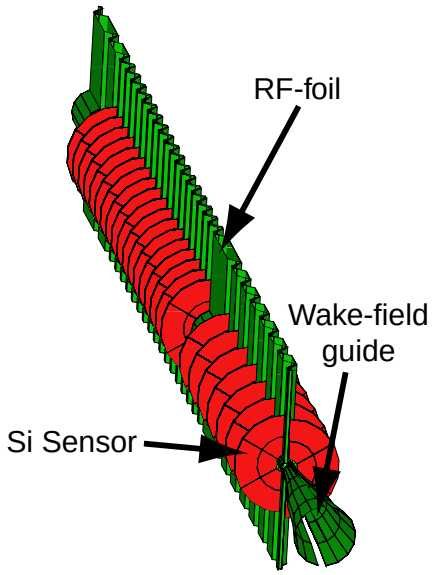

Figure 2: The RF–foil, sensors and wake–field guide of the VELO. The wake–field guide is the conical section at the front of this diagram and those in Figures 1 and 3.

Component	GEANT volume	Material	Thickness [μm]	X_0 [%]
Sensors				
VELO	VSRP	Si	300	0.32
VETO	VPRP	Si	300	0.32
Hybrids and supports				
Base	MODB	Al	10000	11.25
Spring	SPRI	Al	4250	4.78
Base	MPBA	Al	6000	6.75
Long paddle	MFLO	C	500	0.26
Long paddle	MBLO	C	500	0.26
Long paddle	MSI1	C	500	0.26
Long paddle	MSI2	C	500	0.26
Short paddle	MFSH	C	500	0.26
Short paddle	MBSH	C	500	0.26
Short paddle	MSI3	C	500	0.26
Short paddle	MSI4	C	500	0.26
Hybrid	COOL	C	400	0.21
Sensor position	VSPC	vacuum	–	–
Clamp	CLA1	Al	1000	1.12
Clamp	CLA2	Al	1000	1.12
RF–foil	F1LK, etc	Al	250	0.28
RF–box				
Top	RFS1	Al	500	0.56
Bottom	RFS2	Al	500	0.56
Front	RFF1	Al	500	0.56
Front	RFF2	Al	500	0.56
Back	RFB1	Al	500	0.56
Back	RFB2	Al	500	0.56
Sides	RFT1	Al	10000	11.25
Holes	RFT2	vacuum	–	–
Wake field guide	FWAK	Cu	100	0.69
Vacuum tank				
Tank exit foil	VTA3	Al	2650[a]	2.98
Vacuum pipe	PMV1	Al	2000	2.25

[a]Because the foil thickness varies in the GEANT description the value given here is the mean. More details are given in Section 2.5.

Table 1: The material composition, GEANT volume, thickness and X_0 of the VELO components. The thickness refers to the volumes ΔZ. The X_0 corresponds to that of a particle entering the volume normal to the surface.

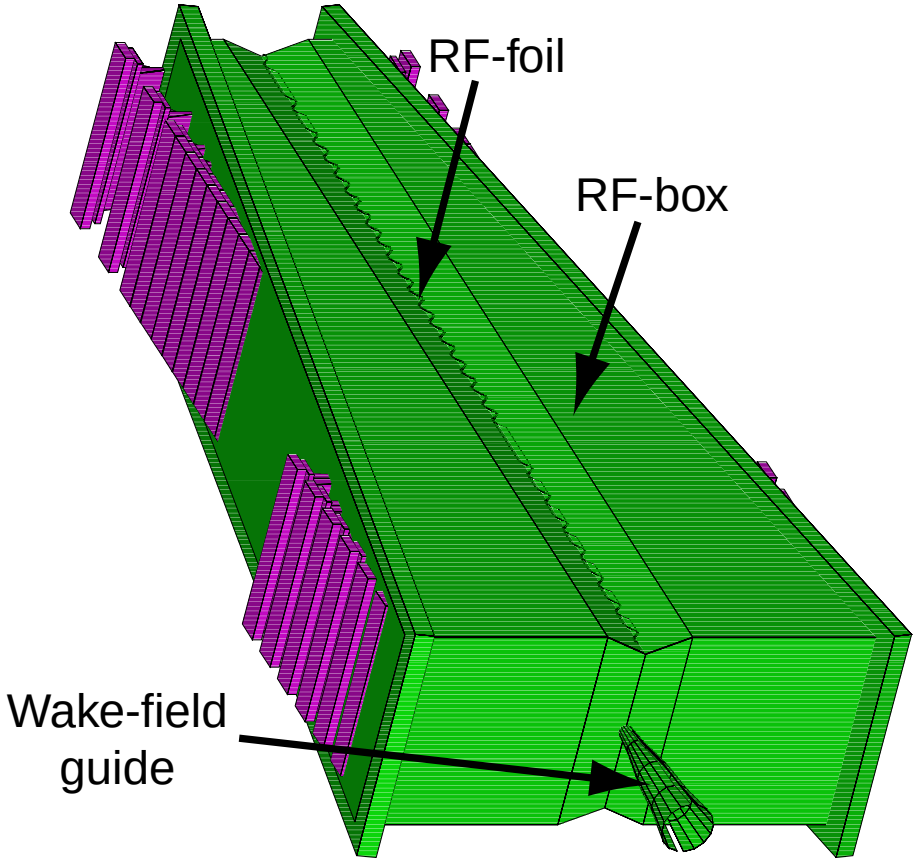

Figure 3: The VELO RF–box. Each half encapsulates half the sensors, hybrids and supports of the VELO.

2.2 The silicon supports and hybrids

The silicon supports come in two varieties: long, for the 7 forward stations, and short for the 18 central stations. In the simulation, the supports are described as: a) a base made of two plates of aluminium with an aluminium spring in between (`GEANT` volumes `MODB`, `MPBA` and `SPRI`); b) a carbon fibre sleeve (or 'paddle') with walls of thickness 500 μm (`GEANT` volumes `MFLO`, `MBLO`, `MSI1` and `MSI2` for the long paddles, and `MFSH`, `MBSH`, `MSI3` and `MSI4` for the short paddles); c) a hybrid made of carbon fibre, thickness 400 μm (`GEANT` volume `COOL`), with a (vacuum) hole cut out for the silicon wafers (`GEANT` volume `VSPC`); d) the hybrid is attached to the paddle with an aluminium clamp (`GEANT` volumes `CLA1` and `CLA2`). Figure 1 gives a view of the modules, together with the silicon detectors; more details of the volumes can be found in Table 1.

2.3 The RF–foil

The complicated RF–foil shape necessitates the definition of many `GEANT` volumes. The foil sections are made from 250 μm thick aluminium. The wake-field cone which joins the RF–foil to the beam pipe is represented by the volume `FWAK`. The wake–field cone is constructed from 100 μm thick copper. Figure 2 shows what this assembly of parts looks like.

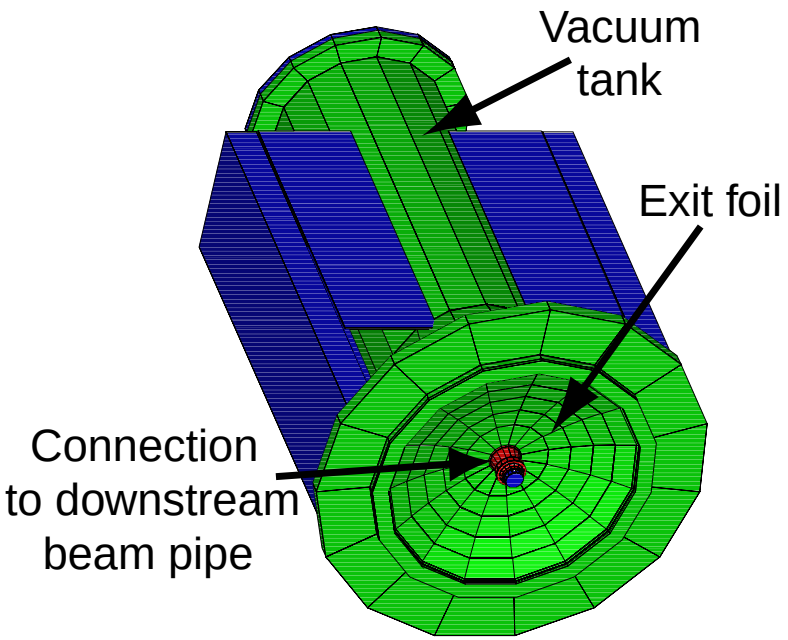

Figure 4: The VELO vacuum tank. The front shows the exit foil and the connection to the downstream LHCb vacuum pipe.

2.4 The RF–box

The box in which the silicon and supports are housed (in a secondary vacuum, separated from the primary LHC vacuum) is called here the 'RF–box'. This box is made of aluminium and has holes in the sides, which are parallel to $y-z$ plane, to allow the insertion of the silicon and the supports. Most of the sides are of 500 μm thick aluminium, with 1 cm thick aluminium flanges on the sides. The `GEANT` description requires the definition of several volumes: a) `RFS1` and `RFS2` for the top and bottom; b) `RFF1`, `RFF2`, `RFB1` and `RFB2` for the front and back; c) `RFT1` for the sides, with `RFT2` being the holes which allow the placement of the silicon in the box. A view of the RF–box can be seen in Figure 3; again, details can be found in Table 1.

2.5 The vacuum tank

The vacuum tank is shown in Figure 4. The only parts of the vacuum tank within the LHCb acceptance are the exit foil and the connection to the vacuum pipe which are at the front of Figure 4. The exit foil is a spherical section with radius of curvature 1 m and is constructed from 2.0 mm thick aluminium. The `GEANT` description of this foil is such

that the thickness of the foil varies. The thickness varies from 1.4 mm to 4.2 mm with a mean value of 2.65 mm. For the region of the exit foil traversed by particles within the acceptance, the thickness varies from 1.4 mm to 2.6 mm with a mean value of 1.8 mm. The foil is represented by the volume `VTA3`. The vacuum pipe connection is constructed of a cone, a cylindrical section and a bellow all constructed from 2 mm thick aluminium. The vacuum pipe connection is defined by the volume `PMV1`.

3 The material distributions in the VELO

This section is divided into two parts. Firstly, the method of calculating the X_0 will be described in Section 3.1. Then the distribution and mean of the X_0 traversed for particles in the acceptance are given in Section 3.2. In addition, the contributions of different components are given and the results in different regions of phase space are discussed.

3.1 The X_0 calculation

The X_0 traversed by a particle can be calculated in `SICB` using the `GEANT` particle type called a 'geantino'. The 'geantino' traverses the material volumes without undergoing any physics interactions. At the boundary of each volume the distance traversed, volume material and volume name are given. From these numbers the X_0 of each step was calculated [2]. The step X_0 values were then used to calculate the number of X_0 traversed along a trajectory and within the different VELO components.

'Geantinos' were produced to scan the pseudo-rapidity (η) and azimuthal angle (ϕ) acceptance. These variables were chosen because the differential cross section:

$$\frac{\mathrm{d}\sigma}{\mathrm{d}\eta \mathrm{d}\phi} \approx \text{constant} ,$$

for pp interactions. Therefore, the mean X_0 in part of the η–ϕ phase space gives an estimate of that traversed by particles originating from a pp interaction.

The 'geantinos' were tracked from the origin along trajectories within the angular ranges $5.5 \geq \eta \geq 2$ and $-90^\circ \leq \phi \leq 90^\circ$. The η range corresponds to 8 mrad $\leq \theta \leq$ 270 mrad which is approximately the LHCb spectrometer polar angle acceptance. The ϕ range covers only half the acceptance however the VELO is nearly symmetric about the $x = 0$ plane as can be seen in Figures 2–4. Therefore, the numbers are applicable for the whole VELO. Within these ranges the number of steps in η and ϕ were 70 and 100 respectively.

The 'geantino' was no longer tracked once it had exited the vertex tank through the foil or had entered the vacuum pipe for one step. The material traversed in the 25 mrad cone of the vacuum pipe was not included in the X_0 numbers presented, though this material is shown in some of the figures for clarity.

3.2 The X_0 distribution results

The 7000 'geantino' trajectories scanned were used to calculate the mean value of the X_0 traversed ($< X_0 >$):

$$< X_0 >= 18.9\% \text{ of an } X_0 .$$

[2] The code used is a modified version of that written by I. Korolko.

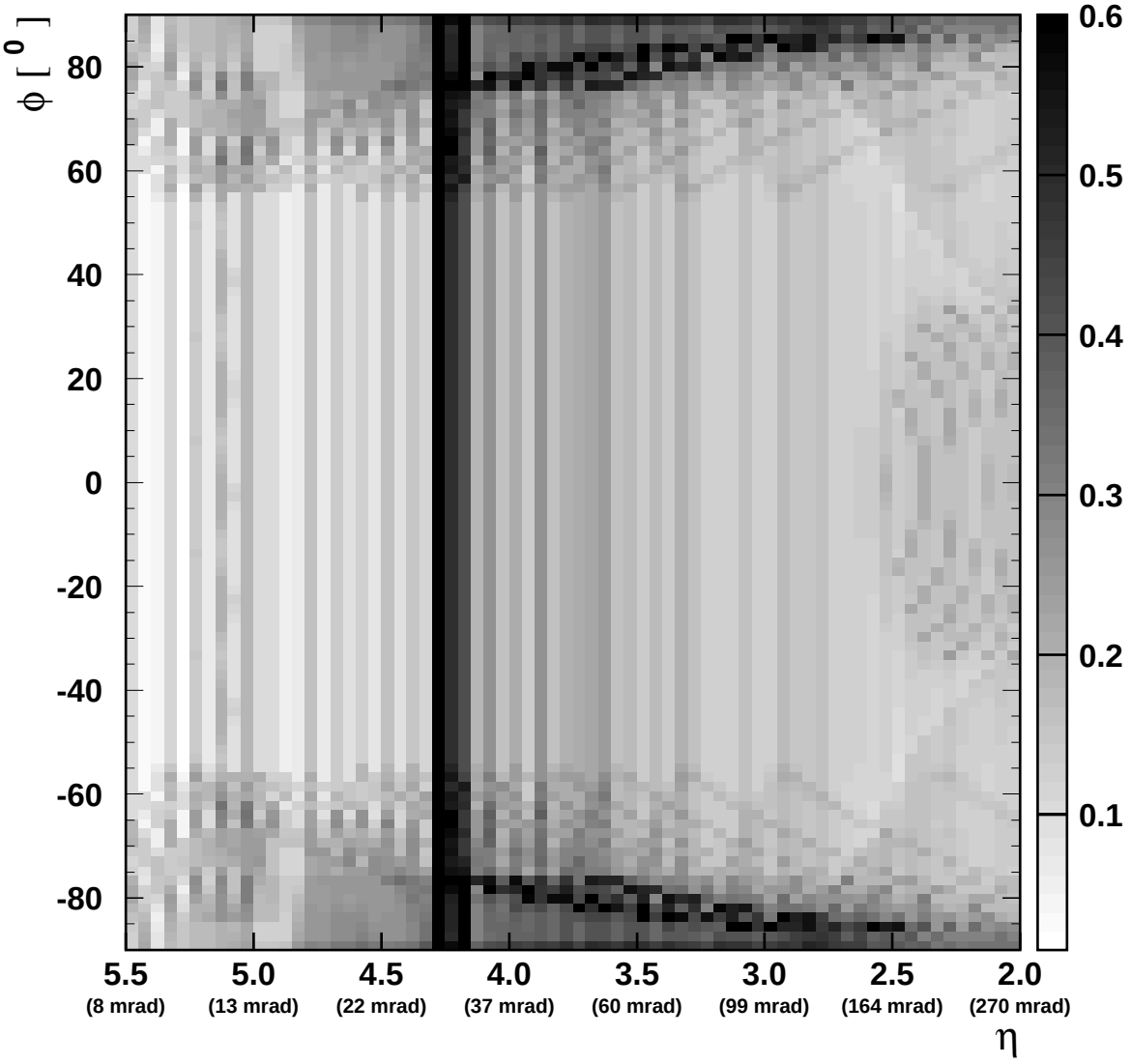

Figure 5: The material distribution traversed for particles of different η and ϕ. The number of X_0 traversed at the exit of the VELO tank is indicated by the scale on the right–hand side of the plot.

Acceptance	X_0[%]		
	All (100% phase space)	$\|\phi\| < 70°$ (78% phase space)	$\|\phi\| > 70°$ (22% phase space)
Total ($< X_0 >$)	**18.9**	**15.9**	**29.5**
Individual components			
Silicon	5.3	5.2	5.7
Hybrid and support	1.4	1.5	1.0
RF–foil	8.2	5.1	19.0
RF–box	0.8	0.7	1.2
Wake–field guide	0.4	0.5	0.3
Vacuum tank	1.9	1.9	1.9
Ambiguously defined[a]	1.0	1.1	0.6

[a]Explained at the end of Section 3.2.

Table 2: The mean X_0 traversed in the VELO and the contribution from different components. The values are given for the total and two different azimuthal acceptances.

The value of $< X_0 >$ calculated for the TP design is 7.5% of an X_0. However, recalling Section 2, the RF–shielding was unrealistic in this design.

The value of $< X_0 >$ and the contributions from the different VELO components over the whole acceptance are given in the second column of Table 2. The most significant contribution is 8.2% of an X_0 from the RF–foil. The silicon contributes 5.3% of an X_0; all other components contribute less the 2% of an X_0 each.

The 2–dimensional distribution of the number of X_0 traversed in the $\eta - \phi$ plane is shown in Figure 5. The scale was truncated at 0.6 X_0. The dark band at $\eta \approx 4.3$ is due to the 25 mrad conical section of the vacuum pipe. The remaining structures observed are due to the components of the VELO. In Figure 6 the X_0 distributions against η and ϕ for each of the VELO components are shown. Each of these distributions are discussed in turn below.

Silicon

The silicon X_0 distribution is given in Figure 6(a). The silicon contribution increases with decreasing η until a maximum occurs at $\eta \approx 3.5$ of $\sim 12\%$ of an X_0, when most forward stations are traversed. There are two bands at $|\phi| = 90°$ where particles traverse the overlapping stations in both halves of the detector and the material traversed is doubled.

Hybrid and support

The hybrid and support X_0 distribution is given in Figure 6(b). The hybrid starts at $r = 4.5$ cm so only particles with $\theta > 60$ mrad traverse the hybrids and/or supports. The contribution is maximised for particles with $\theta > 170$ mrad and $|\phi| < 30°$ where the 'paddles' and clamps contribute to the material traversed.

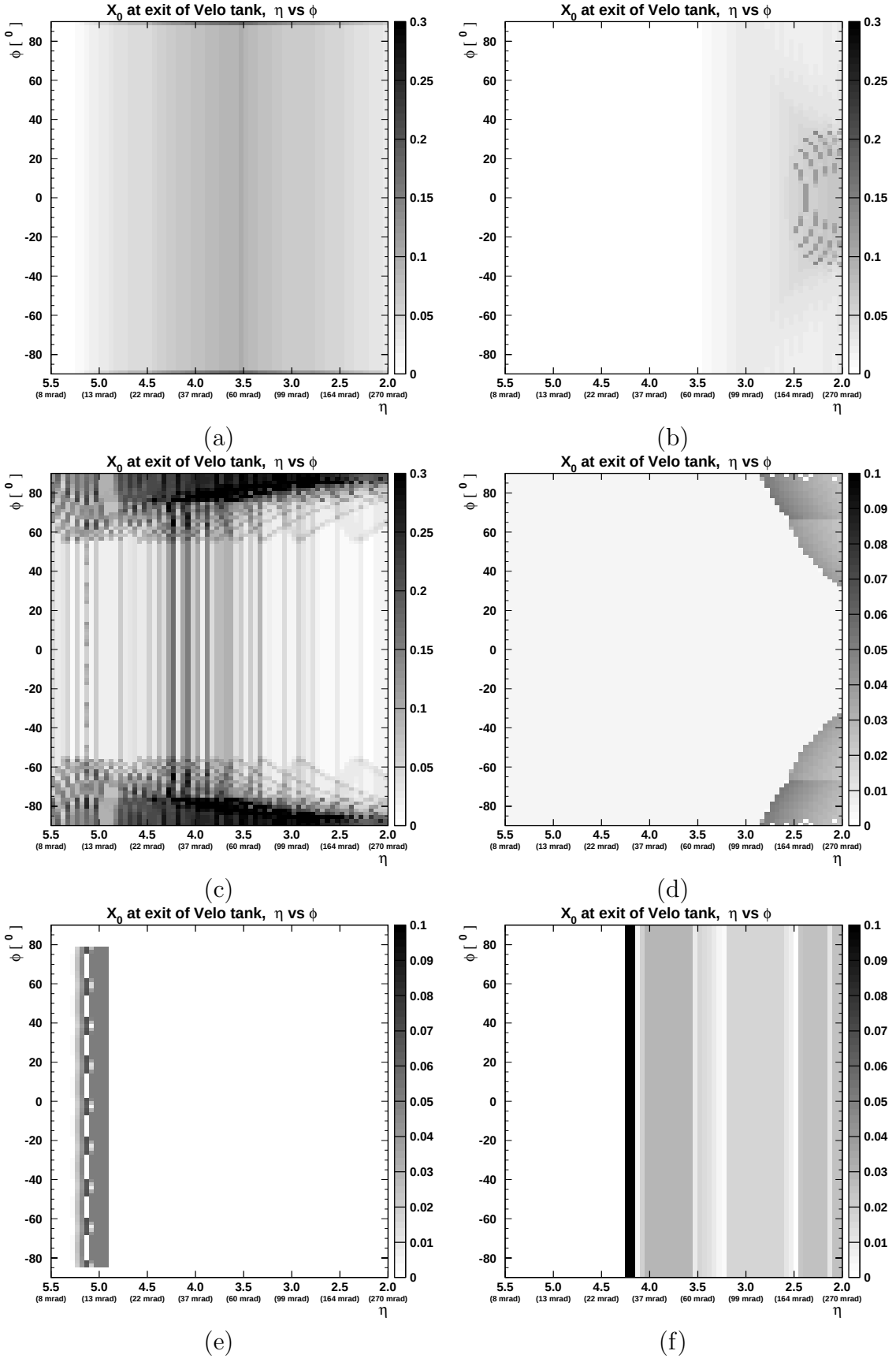

Figure 6: The X_0 traversed (right–hand side scale) for different η and ϕ for different components: (a) the silicon, (b) the hybrid and supports, (c) the RF–foil, (d) the RF–box, (e) the wake–field guide and (f) the vacuum tank.

RF–foil
The RF–foil X_0 distribution is given in Figure 6(c). The RF–foil is the largest contribution to the material traversed in the VELO. The material contribution is maximal in the regions around the $x = 0$ plane ($|\phi| > 70°$) where 50% or more of an X_0 can be traversed in the RF–foil alone. The trajectories with very large contributions are discussed in Section 4.

RF–box
The RF–box X_0 distribution is given in Figure 6(d). The RF–box only contributes significantly at large θ. This could be reduced if the foil and box were made wider.

Wake–field guide
The wake–field guide X_0 distribution is given in Figure 6(e). The copper wake–field only contributes at very low angle in the range $5.25 > \eta > 4.9$ which is only 10% of the acceptance.

Vacuum tank
The vacuum tank X_0 distribution is given in Figure 6(f). The high X_0 band at $\eta \approx 4.25$ is due to the vacuum pipe connection. The X_0 contributions at $\eta < 4.1$ are due solely to the exit foil. The structure seen is an artifact of the implementation in `GEANT` of the spherical section as a series of conical annuli.

Some of the features described above can also be seen in the X_0 distributions of the whole VELO, for fixed values of η or ϕ against the other angular variable; examples are given in Figures 7(a)-(d). In Figure 7 (a), where $\phi = 0°$, the reduced amount of material traversed at high η compared to low η can be seen. The spike at $\eta = 4.25$ is due to the beam pipe. In Figure 7(b) the distribution for $\phi = 80°$ is shown. The large increase in material traversed due to the RF–foil is visible compared to $\phi = 0°$. The maximum, excluding the beam pipe, is at $\eta = 3.75$. The increase in material at $|\phi| > 60°$ is again clearly seen in the slices at $\eta = 4$ and $\eta = 2.5$ in Figures 7 (c) and (d) respectively. In the remaining azimuthal acceptance the distribution is flat at around 16% of an X_0 at $\eta = 4$. For $\eta = 2.5$ an increase around $\phi = 0$ can be seen which is due to the silicon and hybrid supports.

The third and fourth columns of Table 2 give $< X_0 >$, and the contributions from different components, for the trajectories in the azimuthal ranges $|\phi| < 70°$ and $|\phi| > 70°$ respectively. For the RF–shield, the 5.1 % of an X_0 contributed for trajectories with $|\phi| < 70°$, compared to 19.0 % of an X_0 for trajectories with $|\phi| > 70°$, demonstrates the dominance of this component near the $x = 0$ plane. However, the 5.1% seen for trajectories $|\phi| < 70°$ corresponds to 4.5 mm traversed in the aluminium of the foil. This can be understood from Figure 8 which shows the sections of the RF–foil between the silicon planes. These extend to a radius of $\sim$2 cm therefore several of these are traversed by particles in most of the acceptance; each one corresponds to more than 0.5 mm of aluminium. The reasons for this RF–shield design are discussed in Section 5.1.

The material labelled as ambiguously defined in Table 2 were steps in a volume defined

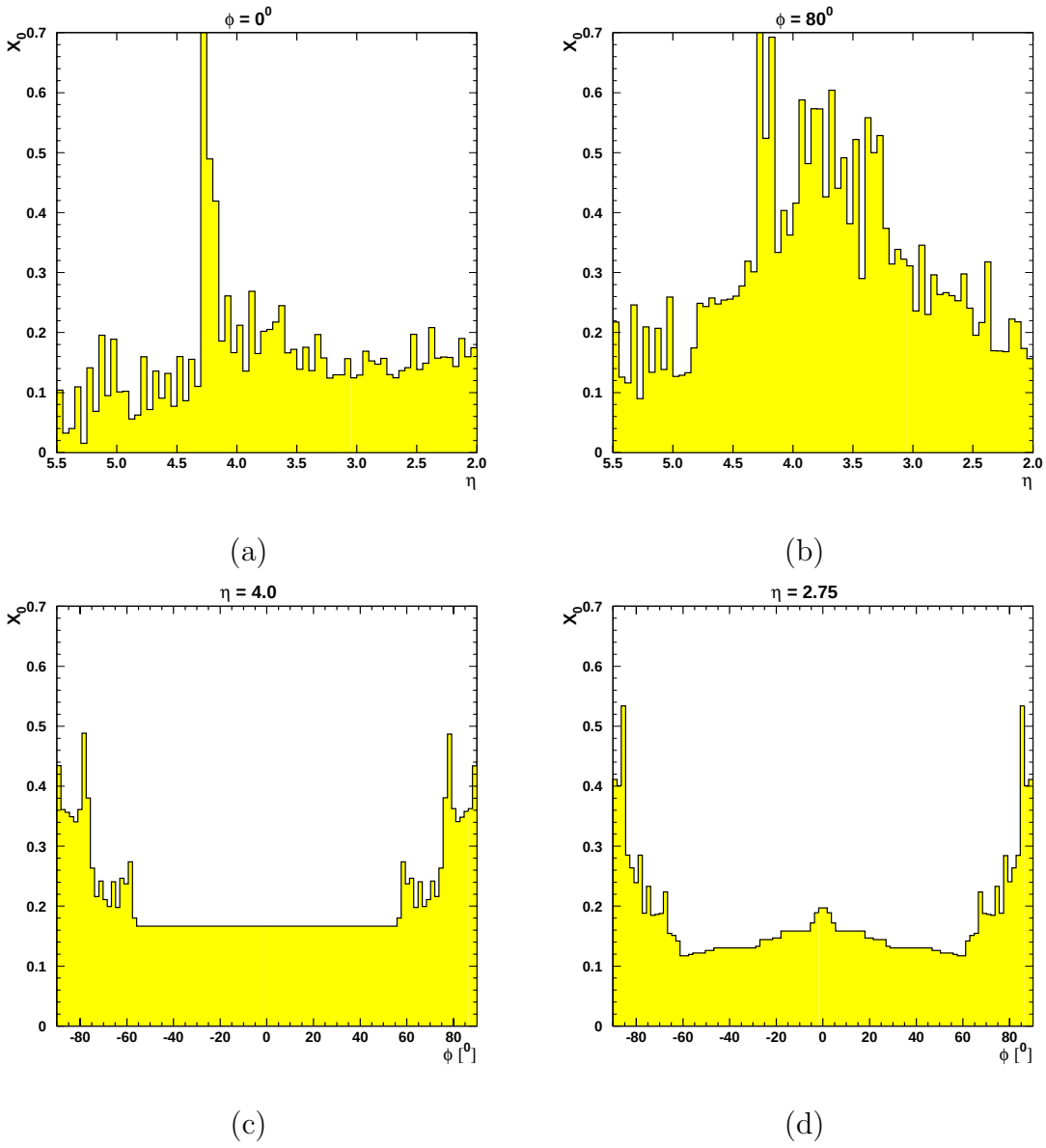

Figure 7: The X_0 distributions at different fixed values of η (ϕ) versus ϕ (η): (a) $\phi = 0°$, (b) $\phi = 80°$, (c) $\eta = 4$, (d) $\eta = 2.5$.

as vacuum in GEANT, but associated with another material. The distribution in η and ϕ of ambiguously defined material is shown in Figure 9. Distributions similar to those of the 'paddles' in Figure 6(b) and the wake–field guide in Figure 6(e) can be seen. For this reason the material is included in the total while investigations in to why this occurs are on going[3]. For this reason the values of $< \mathrm{X}_0 >$ are considered to have an uncertainty of $\sim 1\%$ of an X_0.

4 Phase space regions with large X_0 traversed

Certain trajectories can traverse up to 70% of an X_0 in the VELO. These trajectories are close to the $x = 0$ plane in which the majority of the material of the RF–foil is situated. Typical values of the track angles are $\theta = 40 - 100$ mrad and $|\phi| \approx 80^\circ$. These trajectories traverse more than 5 cm of aluminium (greater than 56% of an X_0) in the RF–foil; the remainder of the material comes from the silicon or hybrids and the exit foil.

The schematic of such a trajectory in the RF–foil is shown in Figure 10. 50% of all the material traversed in the RF–shield ($\sim$2.5 cm) is where the particle exits the RF–foil through one of the flat sections between the very forward stations. In the figure the vertical axis is scaled to be 10 times that of the horizontal axis, so that the flat section traversed by the 'geantino' (indicated by the arrow) as it exits the foil, can be clearly seen. Also visible in this projection are the large number of corrugations traversed due to the overlap of the two foils. This accounts for a further 1.5 cm of the aluminium traversed. The remaining 1 cm arises from the first few traversings of the foil by the 'geantino'. These take place in one or more of the sections which make up the beam pipe through the detectors at low r; these can be seen in Figure 8.

These trajectories are rare, occurring in less than 0.5% of the acceptance. However, trajectories close to these extreme examples help to understand how the average X_0 traversed for $|\phi| > 70^\circ$ is nearly 30 % of an X_0.

5 Possible designs to reduce mean X_0

In this section possible alterations to the VELO and the consequences on the material distribution are discussed: a reduction in the number of stations, a different design for the RF–foil, a reduced thickness of the RF–foil and a reduced thickness of the silicon. This section is speculative and caveats are given for all alterations which might reduce $< \mathrm{X}_0 >$.

5.1 A reduction in the number of stations

The current length of the VELO (the position of the most forward station) is determined by the requirement of three hits on a track from the origin, with a polar angle of 12 mrad. If the most forward station was to become that at z =58.5 cm compared to the current design of z =73.5 cm (the removal of 3 stations) the minimum polar angle acceptance, for a track from the origin, would increase to 16 mrad. The value of $< \mathrm{X}_0 >$ decreases to 14.8 % of an X_0 for such a design.

[3]Problems related to the precision of steps in GEANT tracking are suspected.

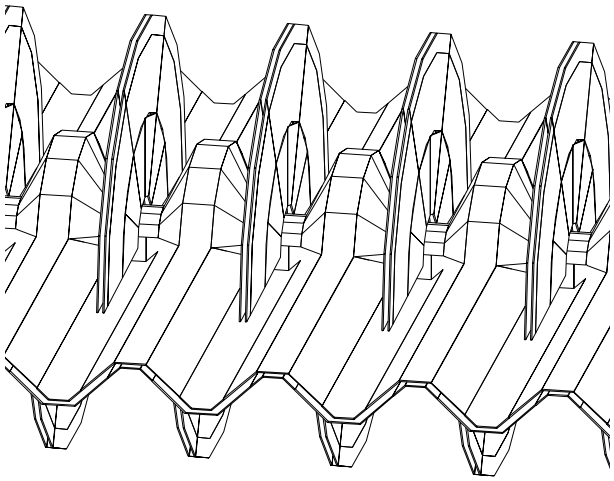

Figure 8: A close up the RF–shield and the silicon planes. The sections between the silicon detectors are traversed several times for particles even if $|\phi| < 70^\circ$, away from the plane containing the flat sections of the RF–shield.

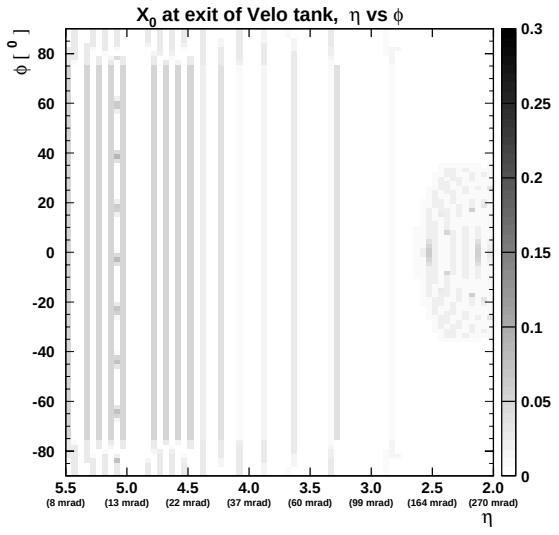

Figure 9: The material distribution traversed for particles of different η and ϕ which was ambiguously defined.

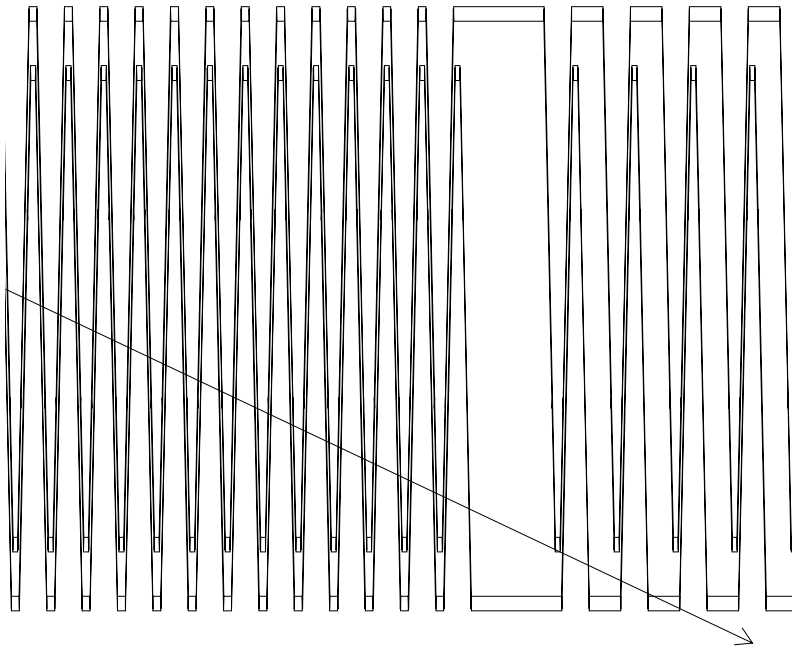

Figure 10: A schematic, in the $x-z$ projection, of a trajectory which traverses more than 5 cm of aluminium in the RF–foil. The vertical scale is 10 times the horizontal scale.

Adopting such a design clearly leads to a loss in acceptance. To calculate this the spread in z of the interaction point about z =0 cm needs to taken into account. The maximum η acceptance of the 'full' and 'short' VELO designs described above are plotted against the origin in z of a track in Figure 11. Convoluting these z dependent acceptance functions with a Gaussian of width 5 cm, which is the interaction point spread in z, yields the mean maximum η acceptance of the VELO design. If the maximum η acceptance of the 'full' VELO is taken to define the acceptance of the rest of the spectrometer the loss of phase space coverage is 8.9% for the 'short' VELO designs. If the maximum η acceptance is taken to be 5.5 the loss is 7.7%.

It is possible that the reduction in acceptance may not be that important because of the reconstruction of low angle tracks downstream. The inner tracker has a minimum rectangular (full minimum polar angle) acceptance of 18.6 (26.3) mrad, 16.0 (22.6) mrad and 14 (19.8) mrad in the magnet stations 2, 3 and 4 respectively [6]. In Figure 11 the mean, maximum and minimum η acceptances of the inner tracker station 3 (IT3) are also shown. There is limited overlap between the 'full' VELO design and the IT3 η acceptance over the $\pm 3\sigma$ interaction point z range shown.

The impact on physics due to the reduction in the VELO acceptance, and its matching with the rest of the spectrometers acceptance, needs to be studied before such a design could be adopted.

The number of stations required would also be decreased by choosing a larger outer radius of the silicon sensors. The limited number of producers of 6" wafers was the reason

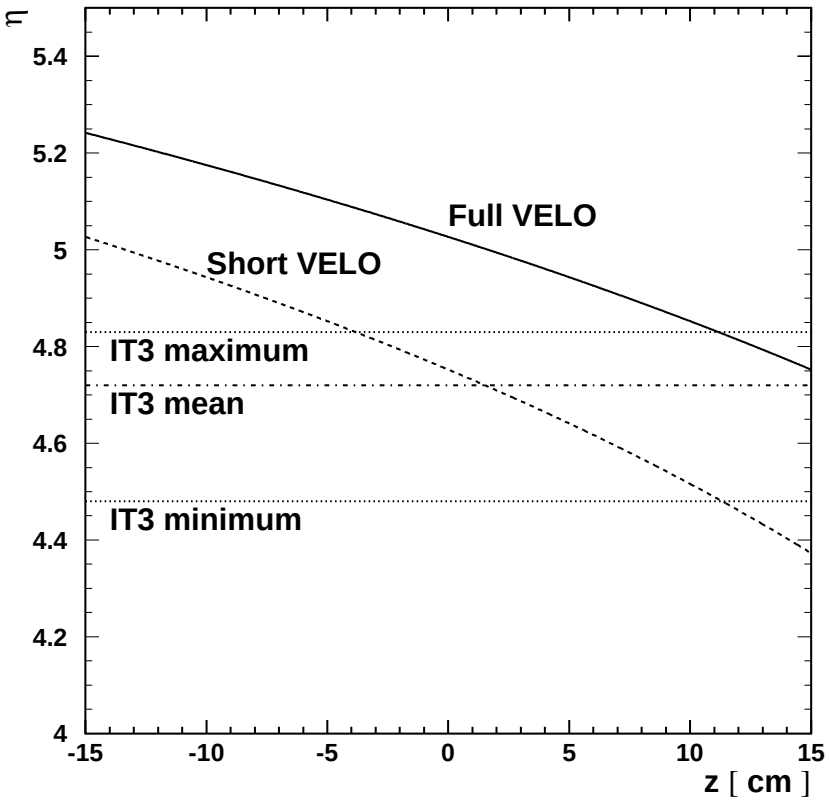

Figure 11: The maximum η at which a track has three VELO hits on a track for the 'full' VELO (solid line) and the 'short' VELO (dashed line), against the primary interaction postion in z in the range -15 cm to 15 cm. The mean η acceptance of the inner tracker station 3 (IT3) (dash and dotted line) and the maximum and minimum acceptances (dotted line) are also shown.

for the outer radius to be limited to 45 mm, the maximum possible from a 4" wafer [1]. Whether this is a possible way of reducing the number of stations, and therefore material, is an open question.

5.2 Alternative RF–foil design

The current 'toblerone' design of the RF–shield was chosen to minimise the material traversed before the first measured point on a track in the VELO. This minimises the multiple scattering leading to the best level–1 trigger performance [7]. The distribution for the 'toblerone' design of the X_0 traversed before the first measured point, against η and ϕ, is given in Figure 12(a). The mean value over the acceptance is 3.2% of an X_0.

An alternative RF–foil is flat with a central semi–cylinder for a beam–pipe. This design would no longer have the problem trajectories related to flat sections (apart from at $|\phi| \approx 90°$) and corrugations in RF–foil described in Section 4. However, there are several drawbacks to this design.

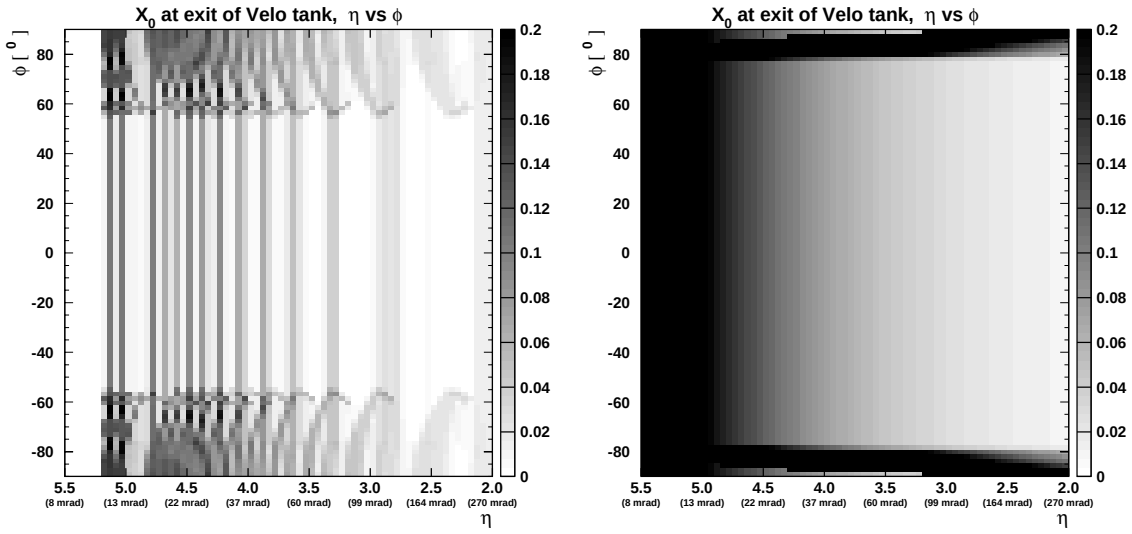

(a) (b)

Figure 12: The X_0 traversed before the first measured point against η and ϕ for: (a) the 'toblerone' RF–foil and (b) the flat RF–foil with beam pipe.

Firstly, the average amount of material before the first measured point increases to a mean value of 12% of an X_0. The distribution of the X_0 traversed before the first measured point for a simple simulation of such a design is given in Figure 12(b). Large parts of the acceptance see more than 20% of an X_0.

There are two other disadvantages: (a) overlap between the detector halves is no longer possible, so there would not be 2π azimuthal coverage; (b) the mechanical strength is less than for the 'toblerone' design.

Another modification to the RF–foil would be to minimise or eliminate the flat sections. However, the current design is yet to be fabricated and designs without the flat sections are more difficult to produce. Once the current design has been fabricated more complex designs, which reduce the flat sections, could be considered.

5.3 A reduction in the RF–foil thickness

The minimum thickness of an aluminium RF–foil which provides the appropriate attenuation is estimated to be 170 μm[8]. If a foil of this thickness was used, the mean contribution of the RF–foil would be reduced to 4.9% of an X_0 and $< X_0 >$ would be 16.6% of an X_0.

The thickness of the foil is not only constrained by the attenuation of the RF–field but also its mechanical strength, in case a pressure differential between the primary (LHC) and secondary (VELO) vacua were to develop [9]. The current design is being discussed with the LHC vacuum group; whether a decrease in thickness is acceptable is at present unknown.

5.4 A reduction in the silicon thickness

The 300 μm thickness of the silicon detectors is the baseline solution for the VELO because n–on–n prototypes of this thickness have been successfully tested and are available [4]. Thinner n–on–n or suitable p–on–n detectors are under study as a possible sensor. If 200 μm thick silicon was used the value of $< X_0 >$ would be 17.1 % of an X_0.

6 Conclusions

With a realistic VELO design the mean number of X_0 traversed before a particle exits the VELO was found to be 18.9 % of an X_0. This is a factor 2.5 greater than the 'unrealistic' design described in the TP. For $|\phi| > 70°$, which corresponds to 22% of the acceptance, the mean is 29.5% of an X_0. The trajectories which lead to these large values are understood and are related to the RF–foil.

Possible alternative designs were considered. A 4% of an X_0 reduction in material could be achieved by reducing the number of VELO stations. The physics impact of the 8.9% loss of VELO acceptance needs to be studied before such a design could be adopted. An alternative RF–foil design might reduce the material traversed before a particle exits the VELO. However, the effect of the four–fold increase in material before the first measured point in the VELO would be detrimental to the level-1 trigger performance. Further 2% of an X_0 reductions in the mean material traversed could be achieved with the use of thinner silicon sensors and aluminium in the RF–foil; however, such thickness reductions may not be technically possible.

References

[1] T. Bowcock *et al* . *LHCb note, LHCb 2000-090 VELO.*

[2] The LHCb Collaboration. *LHCb Technical Proposal. CERN/LHCC/98-4, (1998).*

[3] Geant 3.21. *CERN Program Library Long Write-up W5013.*

[4] T. Ruf. *Plenary presentation in February 2001 LHCb week.*

[5] M. McCubbin *et al* . TDR VELO performance note (in preparation). *LHCb note, LHCb 2001-xxx VELO.*

[6] O. Steinkamp. *LHCb note, LHCb-2000-109.*

[7] T.J. Ketel. *LHCb note, LHCb 2000-019 VELO.*

[8] M. Ferro-Luzzi *et al* . TDR note on RF-shielding calculations (in preparation). *LHCb note, LHCb 2001-xxx VELO.*

[9] M. Ferro-Luzzi. TDR secondary vacuum risk analysis note (in preparation). *LHCb note, LHCb 2001-xxx VELO.*